Smart Structures and Systems, *Vol. 17, No. 6 (2016) 1055-1065*
DOI: http://dx.doi.org/10.12989/sss.2016.17.6.1055

An anisotropic ultrasonic transducer for Lamb wave applications

Wensong Zhou*[1,2], Hui Li[1,2] and Fuh-Gwo Yuan[3]

[1]*Key Lab of Structures Dynamic Behavior and Control of the Ministry of Education, Harbin Institute of Technology, 73 Huanghe Road, Harbin 150090, China*
[2]*School of Civil Engineering, Harbin Institute of Technology, 73 Huanghe Road, Harbin 150090, China*
[3]*Department of Mechanical and Aerospace Engineering, North Carolina State University, Raleigh 27695, USA*

(Received January 24, 2016, Revised April 28, 2016, Accepted April 30, 2016)

Abstract. An anisotropic ultrasonic transducer is proposed for Lamb wave applications, such as passive damage or impact localization based on ultrasonic guided wave theory. This transducer is made from a PMNPT single crystal, and has different piezoelectric coefficients d_{31} and d_{32}, which are the same for the conventional piezoelectric materials, such as Lead zirconate titanate (PZT). Different piezoelectric coefficients result in directionality of guided wave generated by this transducer, in other words, it is an anisotropic ultrasonic transducer. And thus, it has different sensitivity in comparison with conventional ultrasonic transducer. The anisotropic one can provide more information related to the direction when it is used as sensors. This paper first shows its detailed properties, including analytical formulae and finite elements simulations. Then, its application is described.

Keywords: ultrasonic transducer; anisotropic; sensing property; ultrasonic applications

1. Introduction

The structural health monitoring (SHM) methods and techniques have proven useful for the safety control of civil engineering (Basseville *et al*. 2000, Farrar *et al*. 2001, Ye *et al*. 2012, Ye *et al*. 2013), while SHM methods based ultrasonic guided waves theory have proven reliable for the detection, localization and quantification of small structural damages (Cawley and Alleyne 1996, Raghavan and Cesnik 2007, Ma *et al*. 2015). In applications of ultrasonic guided waves, the key device or component is the transducer, which can implement the conversions between guided wave signal and the signal in another measurable form, such as electric signal. The transducers used to generate the guided wave propagating in structures are called ultrasonic actuators or transmitters, while those used to capture the guided waves propagating in structures and convert to measurable signal are called ultrasonic sensors or receivers. Actually, most of transducers can work as these two roles.

In general, guided waves can be actively excited and received through a number of means. The most commonly used transducers are piezoelectric transducers (piezoelectric wafer, piezoelectric wedge transducer, PVDF and Macro Fiber Composites (MFC), *etc*.), electromagnetic acoustic transducers (EMATs), air-coupled techniques, magnetostrictive transducers, and so on. From the

*Corresponding author, Professor, E-mail: zhouwensong@hit.edu.cn

http://www.techno-press.org/?journal=sss&subpage=8 ISSN: 1738-1584 (Print), 1738-1991 (Online)

view of the material properties, most of above transducers can be considered as isotropic guided wave transducers, which can excite uniform Lamb wave around the transducer on the plate. Fig. 1 shows the total displacement distribution of Lamb wave excited by a square PZT. A circular PZT can also excite the same displacement field. They are also considered as omni-directional Lamb wave transducers. Another type of transducer is anisotropic, such as MFC. It consists of unidirectional rectangular piezo ceramic rods sandwiched between layers of adhesive, electrodes and polyimide film, so it can actuate and sense directionally. In addition, most of shear horizontal guided wave transducers are anisotropic, i.e., no omni-directional (Seung *et al*. 2013). In comparison with the isotropic transducer, the guided wave generated or received by anisotropic one contains more information related to the direction or angle. Matt and Scalea (2007) proposed the piezoelectric transducer rosettes to identify passive damage or locate impact loading in anisotropic or geometrically complex structures.

In this work, a single crystal material is proposed to work as the anisotropic transducer because of its anisotropic material properties. Zhou *et al*. (2014) employed the same material, but different cutting direction, to generate and receive shear horizontal wave propagating on the plate, and discussed further its fundamental characteristic when generating and receiving both Lamb wave and shear horizontal wave. This paper will describe this material at first, and then utilize its anisotropic property, combining the blind source separation algorithm, to identify different damages from an overlapped acoustic emission signals.

2. The anisotropic piezoelectric wafer and its model

2.1 The anisotropic piezoelectric wafer

Relaxor-$PbTiO_3$ single crystals, including $Pb(Mg_{1/3}Nb_{2/3})O_3$-$PbTiO_3$ (PMNPT) and $Pb(In_{0.5}Nb_{0.5})O_3$-$Pb(Mg_{1/3}Nb_{2/3})O_3$-$PbTiO_3$ (PIN-PMN-PT), have been extensively investigated in last two decades, due to their superior piezoelectric coefficients (d_{33}>1500 pC/N) and electromechanical coupling factors (K_{33}>90%) when poled along the crystallographic direction [001], which is indicated in Fig. 2. Furthermore, different poling directions can also produce larger piezoelectric coefficients (Zhang *et al*. 2006). It's indicated as yellow square in Fig. 2. Experimental results showed that the [011] direction is another promising poling direction to obtain better multidomain piezoelectric materials (Zhang *et al*. 2006), shown in Fig. 2. Zhang *et al*. (2011) calculated the piezoelectric strain coefficients and dielectric permittivity of a [011] poled PMNPT28 crystals in the original coordinates and presented the corresponding full matrix of material constants.

In short, a PMNPT wafer cut from the plate indicated in Fig. 2 has following elastic compliance matrix (Zhang *et al*. 2011)

$$\mathbf{S} = \begin{bmatrix} 14.4 & -23.6 & 15.5 & 0 & 0 & 0 \\ -23.6 & 58.1 & -37.6 & 0 & 0 & 0 \\ 15.5 & -37.6 & 30.5 & 0 & 0 & 0 \\ 0 & 0 & 0 & 14.7 & 0 & 0 \\ 0 & 0 & 0 & 0 & 101 & 0 \\ 0 & 0 & 0 & 0 & 0 & 18.8 \end{bmatrix} \times 10^{-12}\ m^2/N \tag{1}$$

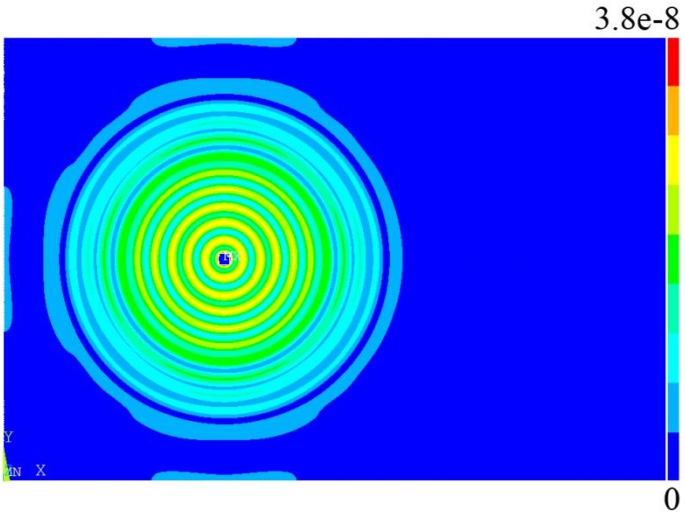

Fig. 1 Total displacement component of Lamb wave excited by a square PZT on the plate (unit: m)

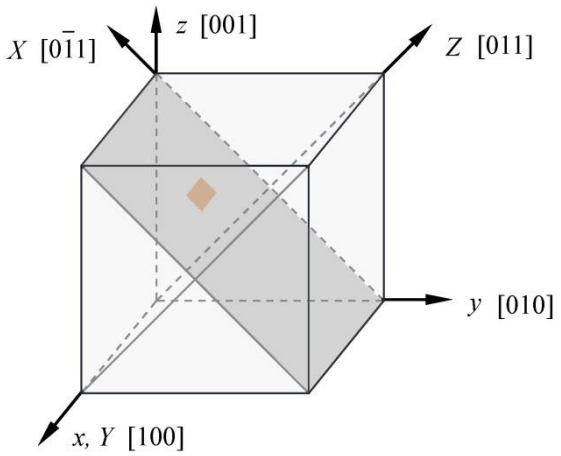

Fig. 2 Poling direction of PMNPT material

While the piezoelectric strain coefficient and dielectric permittivity matrices are expressed as

$$\mathbf{d} = \begin{bmatrix} 0 & 0 & 0 & 0 & 1630 & 0 \\ 0 & 0 & 0 & 239 & 0 & 0 \\ 460 & -1188 & 890 & 0 & 0 & 0 \end{bmatrix} \times 10^{-12}\, C/N \tag{2}$$

$$\epsilon = \begin{bmatrix} 6410 & 0 & 0 \\ 0 & 1470 & 0 \\ 0 & 0 & 3800 \end{bmatrix} \tag{3}$$

At first, from Eq. (1), $S_{11} \neq S_{22}$, $S_{13} \neq S_{23}$, $S_{44} \neq S_{55}$ and $S_{66} \neq 2(S_{11}-S_{12})$, that's different with the conventional transversely isotropic material, such as the PZT. Moreover, From Eq. (2), it can be found that just like the conventional piezoelectric material, there are also five non-zero piezoelectric coefficients, but the difference is all five coefficients are independent and unequal, i.e. $d_{31} \neq d_{32}$ and $d_{24} \neq d_{15}$, which are equal normally for conventional piezoelectric materials. Moreover, in Eq. (3), $\epsilon_{11} \neq \epsilon_{22} \neq \epsilon_{33}$. Above equations indicate that the PMNPT wafer can be considered as the anisotropic transducer, which is expected to exhibit a highly directive response to ultrasonic guided waves. For this wafer, when an external electric field is applied to the wafer in the z direction, the in-plane strain induced by piezoelectric coefficients d_{31} and d_{32} in two directions will be different.

2.2 The modeling of transducer

The thin PMNPT wafer can be considered as plane stress condition. Its coupled electromechanical constitutive equations are written as

$$\begin{aligned} D &= \varepsilon^T E + d\sigma \\ \varepsilon &= s^E \sigma + dE \end{aligned} \tag{4}$$

where D is electric displacement vector, and E the electric field vector. ε and σ are the structural strain and stress respectively. When the direction of external electric field E is along the z-axis and is perpendicular to the surface of the wafer, which is bonded on the surface of plate structure, above equations can be simplified as

$$\begin{aligned} \varepsilon_{11} &= s_{11}^E \sigma_{11} + s_{12}^E \sigma_{22} + E_3 d_{31} \\ \varepsilon_{22} &= s_{12}^E \sigma_{11} + s_{22}^E \sigma_{22} + E_3 d_{32} \\ D_3 &= d_{31}\sigma_{11} + d_{32}\sigma_{22} + \varepsilon_3 E_3 \end{aligned} \tag{5}$$

When the PMNPT wafer works as sensor, and considering the electrical boundary to be the open circuit, the charge on its surface is (Matt and Scalea 2007)

$$\begin{aligned} D_3 = {} & d_{31}s_{11}\varepsilon_{11} + d_{31}s_{12}\varepsilon_{22} + d_{32}s_{12}\varepsilon_{11} + d_{32}s_{22}\varepsilon_{22} \\ & - d_{31}^2 s_{11} E_3 - 2d_{31}d_{32}s_{12}E_3 - d_{32}^2 s_{ss} E_3 + \varepsilon_3 E_3 \end{aligned} \tag{6}$$

According to Matt and Scalea (2007), the voltage response of the proposed PMNPT sensor can be expressed as

$$V = \frac{t\iint\left[d_{31}s_{11}\varepsilon_{11} + d_{31}s_{12}\varepsilon_{22} + d_{32}s_{12}\varepsilon_{11} + d_{32}s_{22}\varepsilon_{22}\right]\mathrm{d}x\mathrm{d}y}{A\left[\varepsilon_3 - \left(d_{31}^2 s_{11} + 2d_{31}d_{32}s_{12} + d_{32}^2 s_{22}\right)\right]} \tag{7}$$

where A is the area of the wafer.

3. FE analysis of the PMNPT wafer in guided wave application

3.1 The deformation under the constant electric field

Finite element simulation can provide clear and intuitive deformation of the proposed wafer under the external voltage. COMSOL Multiphysics is used to obtain the total displacement contour under the constant electric fields for the conventional PZT and the proposed PMNPT wafer, which are shown as Fig. 3. The conventional PZT has uniform deformation with respect to all directions, but the proposed PMNPT deforms unequally along two principal axes for both square and round wafers. The deformation is larger along the y direction than the x one, because of the larger piezoelectric coefficient d_{32}, and also the different sign between d_{31} and d_{32}. Moreover, from Fig.3 the PMNPT wafer has larger deformation relative to the conventional PZT because of its larger piezoelectric coefficients.

3.2 *The impedance characteristics*

ANSYS is employed to obtain the impedance characteristics of the PMNPT wafer. The wafers are modelled with different side length and thickness. The impedance characteristics as a function of frequency for the PMNPT wafer with different size are shown in Fig. 4. For the smaller wafer, the strong vibration was found to occur at higher frequency, while the larger one the lower frequency. The thickness has less effect on the proposed vibration modes.

3.3 *Guided wave excited by the PMNPT wafer*

ANSYS is employed again to analyze the ultrasonic guided wave generation and propagation, induced by the proposed PMNPT wafer, which is bonded on the surface of an aluminum plate. The plate (180 mm × 180 mm × 1 mm) is modeled by the SOLID185 element in ANSYS, while the PMNPT wafer (4 mm × 4 mm × 0.2 mm) is modeled by the SOLID5 element, which has 3-D piezoelectric and structural field analysis capability with coupling between the fields. Material properties shown as Eq. (1)-(3) are assigned to the PMNPT wafer in the finite element model. Between the PMNPT wafer and the plate, there is no adhesive layer, i.e. the ideal coupling contact, in this work. Fig. 5 shows the position of wafer on the plate, in which the 70 mm distance away from the edges can avoid effects of the reflection signals.

The external voltage applied on the PMNPT wafer is a 5-cycle sinusoid tone burst signal with a fixed center frequency 160 kHz. This signal is defined by Eq. (8). It is a narrow band signal, which can reduce the dispersive effects during the guided wave propagation.

$$V_{in}(t) = P[H(t) - H(t - 5/f_c)](1 - \cos\frac{2\pi f_c t}{5})\sin 2\pi f_c t \tag{8}$$

where P is the amplitude of the signal, f_c is the center frequency and $H(t)$ is a Heaviside step function.

Fig. 6 shows the displacement field of guided waves excited by the PMNPT wafer on the top surface of the aluminum plate at 30 μs after the excitation. Both figures are plotted in the local cylindrical coordinate that original point is the center of the wafer. Namely, the directions of both particle displacement components and wave propagation are the radial direction. These two displacement components indicate that the Lamb wave are able to be generated and propagates in the plate. Moreover, from Fig. 6, it can be found that the amplitude of Lamb wave is dependent on the angle of wave propagation, which is different to Fig. 1.

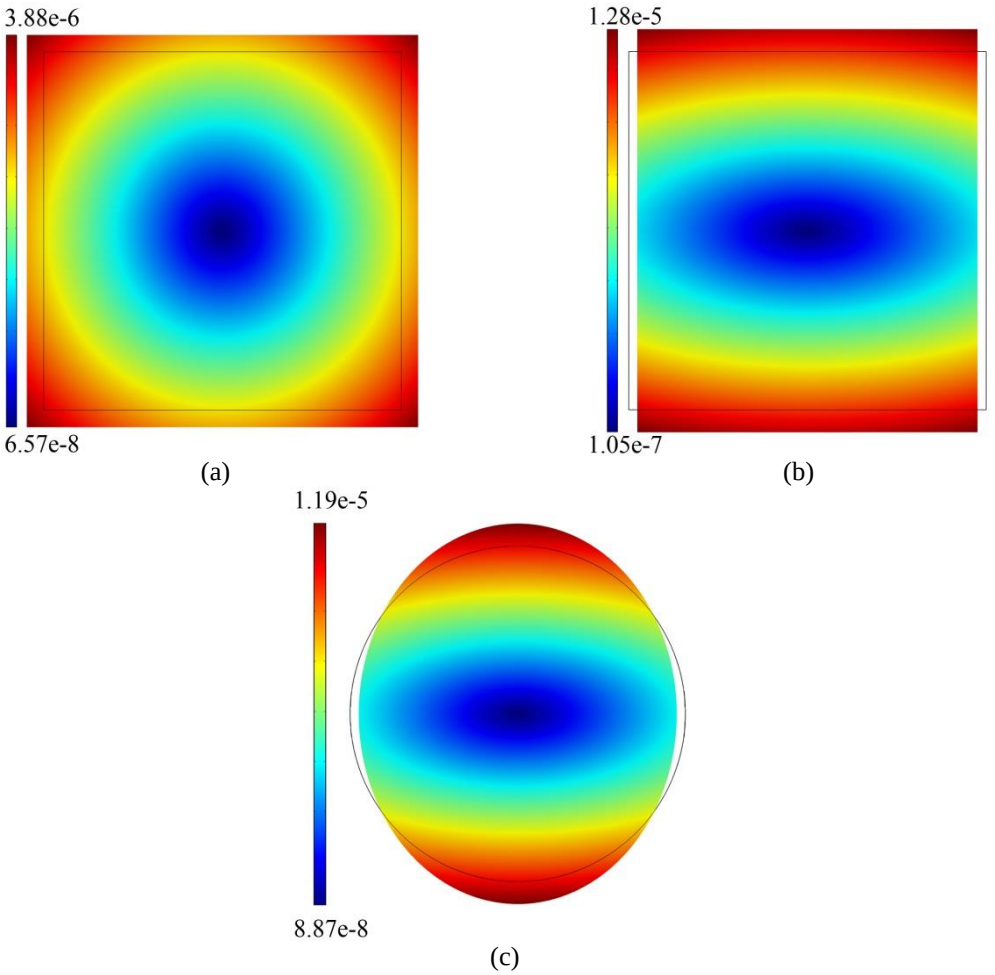

Fig. 3 Deformation under the constant electric fields: (a) conventional PZT, (b) squre PMNPT wafer, and (c) round PMNPT wafer

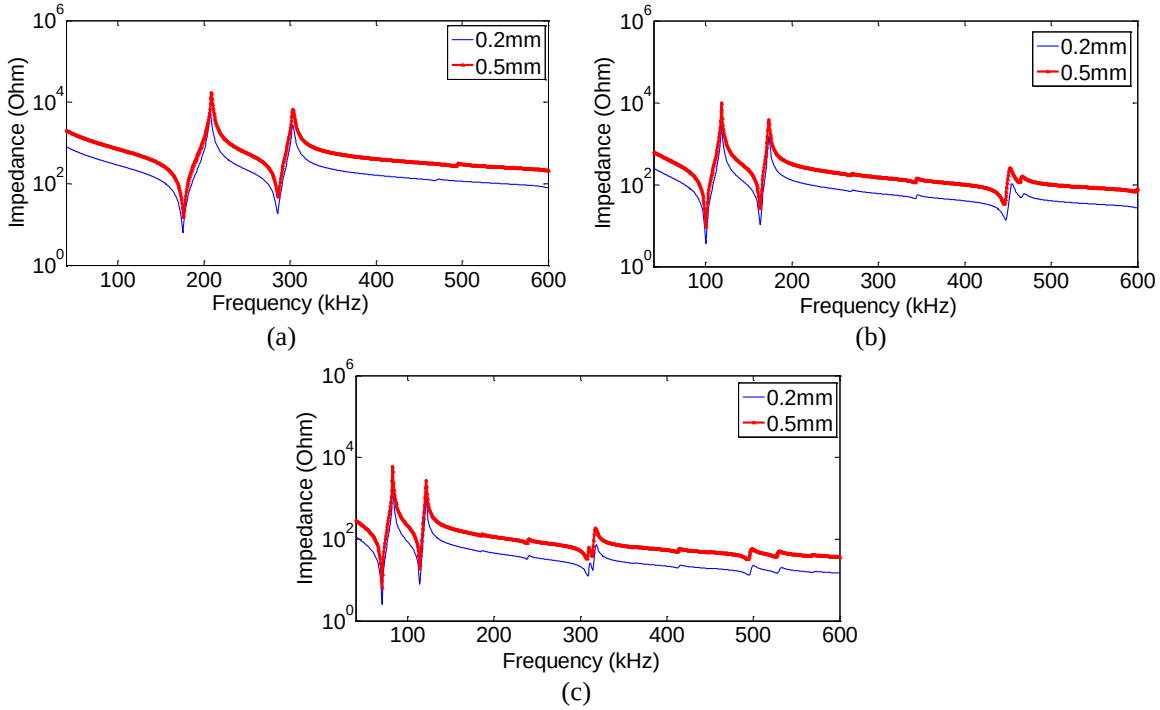

Fig. 4 The impedance curves of the PMNPT wafer with different size: (a) 4 mm×4 mm, (b) 7 mm×7 mm, and (c) 10 mm×10 mm

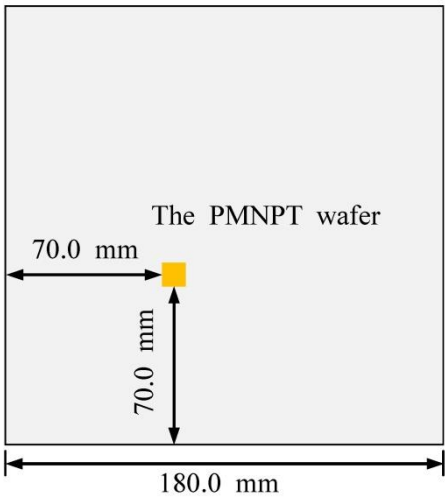

Fig. 5 Layout of the PMNPT wafer and the plate

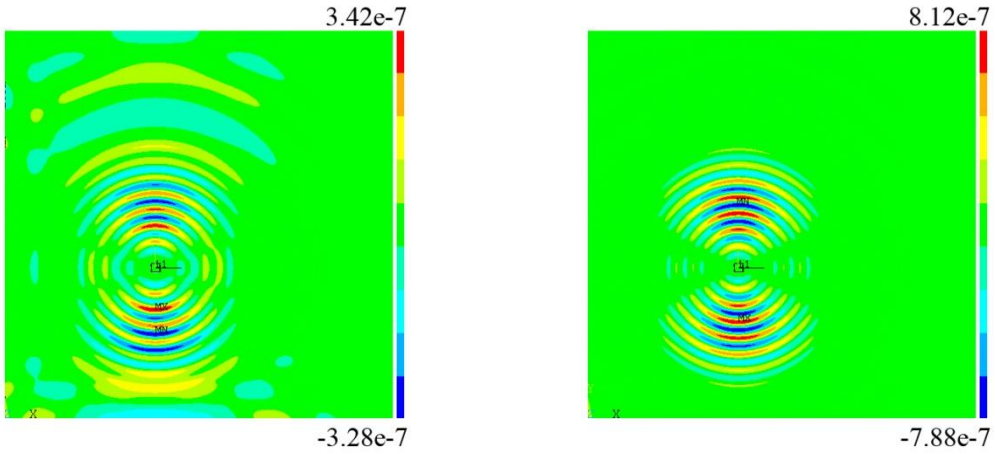

(a) (b)

Fig. 6 Displacement field in local coordinate induced by the PMNPT wafer: (a) displacement component *u* in *x* direction and (b) displacement component *w* in *z* direction

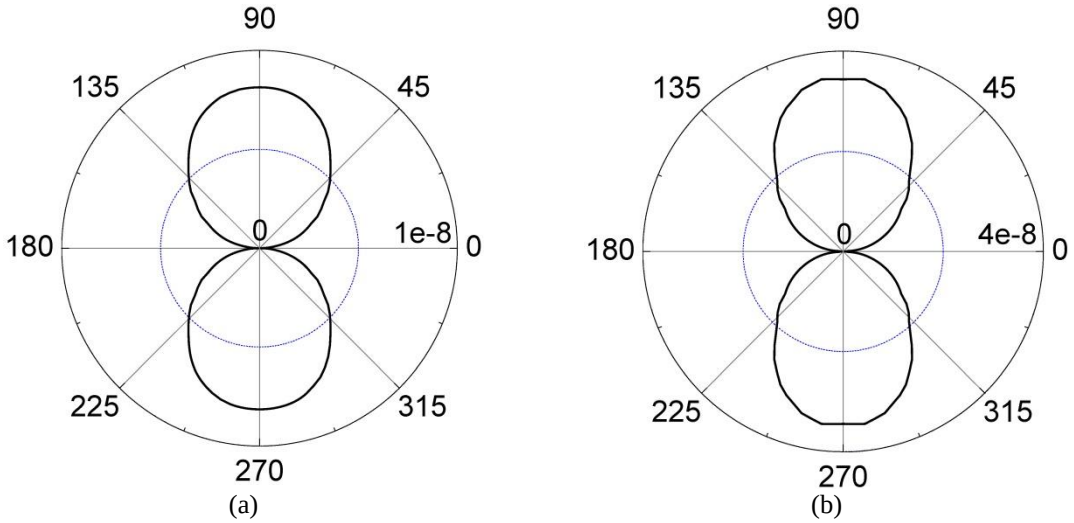

(a) (b)

Fig. 7 Displacement amplitude versus direction of wave propagation: (a): displacement component *u*, (b) displacement component *w* (the angular unit is degree, the displacement unit is m)

Absolute values of the maximum amplitude of these two displacement components are plotted versus the angle of wave propagation, shown as Fig. 7, in which the curves are extracted at the point 60 mm away from the wafer and at different time. Displacement component *u* is predominant for S_0 mode Lamb wave, while displacement component *w* is predominant for A_0 mode Lamb wave. The former has larger group velocity. Moreover, they just show the relative magnitude of Lamb waves' amplitude in various angles. Both Figs. 6 and 7 indicate that Lamb wave with maximum amplitude propagates along the *y* axis, while the minimum amplitude the *x* axis. According to FE analysis, it's also known that the proposed wafer can be the anisotropic

sensor that has various responses to guided waves from different directions.

3.4 Voltage responses of the PMNPT wafer

The voltage responses of the proposed wafer were obtained with finite element analysis too. Unlike the displacement responses, which in *x* and *y* directions can be extracted respectively, the voltage responses contain S_0 and A_0 modes of Lamb wave simultaneously. Therefore, for the simulation in this section, a large Aluminum plate (360 mm × 360 mm × 1 mm) was used to avoid the overlapping signal from reflected guided waves. Fig. 8 shows the voltage responses of the PMNPT wafer in 1/4 quadrant for both S_0 and A_0 modes of Lamb wave, respectively. The similar with the displacement responses, the voltage responses of S_0 and A_0 mode also reach the maximum value along the *y* axis. In the other words, the main energy propagates along the *y* axis.

4. The application of anisotropic transducer

Anisotropic ultrasonic transducer can provide more information about the wave signals than the conventional transducers. Matt and Scalea (2007) investigated the directivity of the MFC response, and employed MFC rosettes to obtain the wave source location. In comparison with the MFC transducer, the proposed wafer has smaller size, and can be also used as rosettes.

The proposed PMNPT wafer is also used to separate the overlapped signals in multiple damage sources problem, with help of blind source separation (BSS) method. The multiple damage sources problem means that several acoustic emission signals are generated from multiple damage sources and overlapped each other during propagation (Nasser and Zhou, 2011). In this case, each guided wave sensor receives the overlapped signals containing information of different damage sources. This situation may be instanced by Fig. 9.

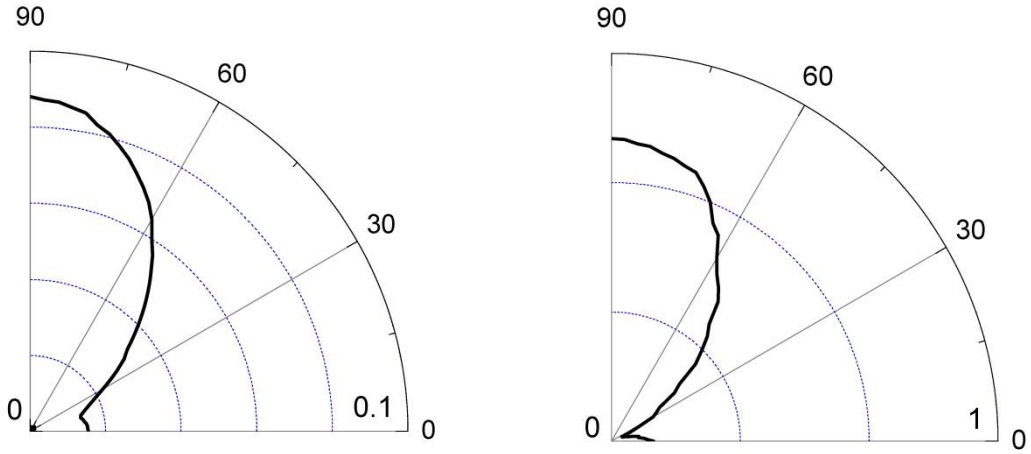

(a) (b)

Fig. 8 Voltage amplitude versus direction of wave propagation: (a): S0 mode and (b) A0 mode (the angular unit is degree, the voltage unit is V)

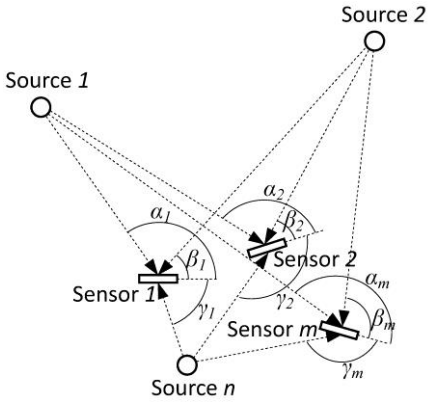

Fig. 9 Piezoelectric sensors and multiple damage sources (Nasser and Zhou 2011)

Assume that signals denoted by s_1, s_2 … s_n are generated from n sources, and m sensors are fixed at different orientations to catch m orthogonal overlapped signals denoted x_1, x_2 … x_m. The signal mixing procedure may be expressed as the linear equations

$$\begin{aligned} x_1 &= a_{11}s_1 + a_{12}s_2 + \cdots + a_{1n}s_n \\ x_2 &= a_{21}s_1 + a_{22}s_2 + \cdots + a_{2n}s_n \\ &\cdots \\ x_m &= a_{m1}s_1 + a_{m2}s_2 + \cdots + a_{mn}s_n \end{aligned} \tag{9}$$

where a_{11}, a_{12}, a_{21}… a_{mn} are the parameters that depend on the location/orientation of the sensor and their properties as well. Anisotropic sensor can provide different coefficients a_{11}, a_{12}, a_{21} … a_{mn} due to their directivity. Nasser and Zhou (2011) employed independent component analysis, i.e. BSS method to solve Eq. (9) and recovered the original signals from each signal source. Since the proposed wafer is the anisotropic sensor, they are also used to implement above signal separation procedure.

5. Conclusions

In this work, an anisotropic transducer made of PMNPT single crystal was proposed to generate and receive Lamb wave. The PMNPT wafer, which is cut in a special direction with respect to its growth direction, has anisotropic elastic and piezoelectric coefficient matrices. The deformation under the constant electric field and the impedance characteristics are obtained using finite element analysis. Subsequently, finite element simulation on a plate also indicates that Lamb wave excited by this wafer is not uniform around the wafer. It has maximum displacement response along one axis, while minimum another axis. For the applications, the wafer is proposed to obtain the damage or impact location by rosettes, and also implement the signal separation procedure in multiple damage sources problem.

Acknowledgments

The financial support from the National Science Foundation of China under Grant No. 51578191 and the National Key Technology R&D Program under Grant No. 2014BAG05B07 are gratefully appreciated.

References

Basseville, M., Abdelghani, M. and Benveniste, A. (2000), "Subspace-based fault detection algorithms for vibration monitoring", *Automatica*, **36**(1), 101-109.

Cawley, P. and Alleyne, D. (1996), "The use of Lamb waves for the long range inspection of large structures", *Ultrasonics*, **34**, 287-290.

Farrar, C.R., Doebling, S.W. and Nix, D. (2001), "Vibration-based structural damage identification", *Philos. T. Roy. Soc.: Mathematical, Physical and Engineering Sciences*, **359**(1778), 131-149.

Ma, S., Wu, Z., Wang Y. and Liu K. (2015), "The reflection of guided waves from simple dents in pipes", *Ultrasonics*, **57**, 190-197.

Matt, H.M. and Scalea, F.L. di, (2007), "Macro-fiber composite piezoelectric rosettes for acoustic source location in complex structures", *Smart Mater. Struct.*, **16**, 1489-1499.

Nasser, H. and Zhou, W. (2011), "Multi-source acoustic emission signals analysis based on blind source separation using macro fiber composite", *Proceedings of the 8th International Workshop on Structural Health Monitoring*. September 2011, Stanford University, US.

Raghavan, A. and Cesnik, C.E.S. (2007), "Review of guided-wave structural health monitoring Shock", *J. Vib. Dig*. **39**, 91-114.

Seung, H.M., Kim, H.W. and Kim, Y.Y. (2013), "Development of an omni-directional shear-horizontal wave magnetostrictive patch transducer for plates", *Ultrasonics*, **53**, 1304-1308.

Ye, X.W., Ni, Y.Q., Wai, T.T., Wong, K.Y., Zhang, X.M. and Xu, F. (2013), "A vision-based system for dynamic displacement measurement of long-span bridges: algorithm and verification", *Smart Struct. Syst.*, **12**(3-4), 363-379.

Ye, X.W., Ni, Y.Q., Wong, K.Y. and Ko, J.M. (2012), "Statistical analysis of stress spectra for fatigue life assessment of steel bridges with structural health monitoring data", *Eng. Struct.*, **45**, 166-176.

Zhang, R., Jiang, B., Jiang, W. and Cao, W., (2006), "Complete set of elastic, dielectric, and piezoelectric coefficents of 0.93Pb(Zn1⁄3Nb2⁄3)O3–0.07PbTiO3 single crystal poled along [011]", *Appl. Phys. Lett.*, **89**(24), 242908.

Zhang, S., Jiang, W., Meyer, R.J., Li, F., Luo, J. and Cao, W. (2011), "Measurements of face shear properties in relaxor-$PbTiO_3$ single crystals", *J. Appl. Phys.*, **110**, 064106.

Zhou, W., Li, H. and Yuan, F.G. (2014), "Guided wave generation, sensing and damage detection using in-plane shear piezoelectric wafers", *Smart Mater. Struct.*, **23**(1), 015014.